Volume 9, Number 1 (February 2016) p. 22 - 47 • ISSN 1983-4195
http://dx.doi.org/10.1590/S1983-41952016000100003

REVISTA IBRACON DE ESTRUTURAS E MATERIAIS
IBRACON STRUCTURES AND MATERIALS JOURNAL

Analytical model for assessing of strengthening the flexural beams with T and rectangular section

Modelo analítico para avaliação do reforço à flexão de vigas com seção retangular e T

I. ANDREOLLI [a,b]
andreolli@petrobras.com.br
ivandreolli@gmail.com

Abstract

This study presents an analytical model for evaluation of the reinforced beams under simple bending based on recommendations of the Brazilian Concrete Code (NBR-6118) and a study published by the International Federation of Concrete (fib). In this paper are considered two different section types, rectangular and "T" sections and the beam´s deformation are analyzed considering the moment-curvature diagram taking into consideration the limits of deformation of materials. The results obtained by both Codes are confronted each other, showing great similarity. Additionally, destructive tests of reinforced beams have been made in the laboratory and were compared to results obtained by the analytical model, showing excellent performance of the proposed model. The objective of this publication is to present the analytical model. Analysis comparing the field results and the analytical model were presented in another publication mentioned in this study.

Keywords: CFRP, analytical model, reinforced beams, fib, NBR-6118.

Resumo

Este estudo apresenta um modelo analítico para avaliação do reforço de vigas sobre flexão simples com base nas recomendações da Norma Brasileira de Concreto (NBR-6118) e de um estudo publicado pela Federação Internacional do Concreto (Federation International of Betton-fib). São consideradas no estudo seções do tipo retangular e T e as deformações das vigas são analisadas considerando o diagrama momento - curvatura respeitando os limites de deformação dos materiais no estado limite último. Os resultados obtidos por ambas as normas são confrontados entre si, mostrando grande similaridade. Além disso, ensaios destrutivos de vigas reforçadas realizados em laboratório foram confrontados com os obtidos pelo modelo analítico, mostrando excelente desempenho do modelo proposto. O foco dessa publicação está na apresentação do modelo analítico. As análises confrontando os resultados de campo com o modelo analítico foram apresentadas em outra publicação citada nesse estudo.

Palavras-chave: PRFC, modelo analítico, vigas reforçadas, fib, NBR-6118.

[a] *Petróleo Brasileiro S.A. - PETROBRAS, Santos,SP, Brasil;*
[b] *Universidade Santa Cecília - UNISANTA, Santos, SP, Brasil.*

Received: 04 Aug 2015 • Accepted: 01 Dec 2015 • Available Online: 27Jan 2016

1. Introduction

The evaluation of the conservation state and the reparation or the reinforcement of the existing buildings has been recognized as important to economic grown, showing the interest on preserve and rehabilitate the built patrimony. The technological innovation and the development of new materials have dominate this area showing an innumerous challenges and possibilities. Civil structures along the time suffer damages that implies, normally, in a reduction on it's structural capacity and the structural reinforcement might appear as a technical and economical solution (Spagnolo, et al. [1]). A typical example of the reduction in carry capacity of structures happen due to reinforcement oxidation. (Saadatmanesh and Ehsani, [2]; An, et al. [3]). In fact, the reinforcement might contribute to the corrosion. Recently, studies on strengthening techniques, such as, carbon fiber addition to the concrete matrix have shown that could increase structure porosity as well as reinforcement corrosion (Garcés, et al. [4]).

In some circumstances, the structures are submitted to different loads on the project phase, whether by operational errors or project mistakes, as well as by changes in the structure conception regard to the necessity of the modification of usage. In addition a specific project analysis may result in the necessity of reinforce structures in order to become safer and trustable to use (Beber, et al., [5] and Beber, [6]). Must be evaluated the tendency of failure and the limit strain to reinforce the structure. Particularly in case of beam structures, is known that many geometric and physic parameters have influenced in its behavior, consequently, in the strengthening performance, such as: strengthened thickness "section", resistance, types of strengthening, application techniques and others revealed by (An, et al. [3]; Garcez, et al. [7]; Ferrai and Hanai [8]). Innovations in this area have allowed the improvement of application techniques (Tian, et al. [9] and Santos, et al. [10]). However, combination among strengthening types and new materials have allowed new applications in reinforced concrete, such as: strengthening in punching slabs (Santos, et al. [10]), reinforcement in terms of shear stress (Gamino, et al. [11]), prestressed strengthening (Garcez, et al. [12]) and the reinforcement by adding carbon fibers in concrete (Garcés, et al. [4]).

In the application of new techniques and new materials to structural reinforcement is also important to consider the reinforcement structure behavior as long as increase in loads occur, in order to evaluate structural performance. To reinforced concrete or longitudinal and transversal steel bars in beams, the stress-strain diagrams are acknowledged as well as limits deformation. For these structure types there are standards for project implementation. Depending on reinforcement rate, the structure might present a behavior that is not recommended in terms of economical and safety reasons for a project (Beber and Campos, [13]). In terms of reinforcement, there are few code recommendations, mainly when considered reinforcement with technologies such as carbon fiber reinforced polymers (CFRP) and recent application techniques as shown by (Santos, et al. [10] and Yaqub and Bailey [14]).

To project a reinforcement system implies on the adoption of suitable theoretical models, which allow simulating precisely the behavior of the reinforcement elements (Swamy, et al. [15]; Bono, et al. [16]; Gamino, et al. [17]). Experimentally, was verified that reinforced concrete beams behavior, strengthened with composites of carbon fiber, presents features whose observance has vital importance for the appropriate strengthening function (Beber [6]; Andreolli, et al. [18]; Spagnolo, et al. [1]). To simulate and comprehend this behavior, the applied methodology consisted to build moment-curvature diagram, generated by the data that were obtained through a numerical model, a similar methodology is observed in (El-Refaie, et al. [19]; An, et al. [3]; Al-Saidy, et al. [20]), however the full model is not represented in these publications. The model proposed in this work takes in consideration reinforced concrete beams with rectangular and "T" cross-sections, which are submitted to simple bending. The diagrams allows analyzing the beams' behavior as a monolithic structure as new increments of loads are added and allowing evaluating the structure stiffness with or without strengthening. A parametric study, for example, changing the reinforcement rate might show the gain rate of stiffness with a reinforcement increase. Thereby can be conclude which way is more efficient to reinforce and predict beams' behavior. These diagrams are composed in tools to assess the materials performance that composes these type of beams, predicting the possible rupture type of these materials before the sudden rupture, (El-Refaie, et al. [19]; Hollaway and Leeming [21]; Al-Saidy, et al. [20]; Agbossou, et al. [22]).

The moment-curvature diagram analysis was also made by (Andreolli et al. [18]) showing great accuracy between theoretical and experimental data, where also were confronted the recommendations from (NBR-6118, [23]) and fib, [24]). The actual study shows the mathematical model proposed by Andreolli, et al. [18] and developed in order to analyze the behavior of the reinforced concrete beams with carbon fibers or steel plates, through the recommendations of fib [24] and NBR-6118 [23]. It is presented the group of equations in analytical model to determine the position of the neutral line as a function of specific material strain that composes the section submitted to a bending moment, fundamental variable in order to acquire the moment - curvature diagrams. Besides, are presented correlated equations that composes the numerical model.

2. Methodology

To assess the reinforcement behavior, a mathematical model was developed taking into consideration the concrete stress-strain diagram of concrete (σ_c x $\varepsilon(y)$) from the NBR-6118 and fib codes, which are applied to any concrete class strain domain until C50. The model was developed for rectangular and "T" cross section beams. The model was based on the following hypothesis: (i) until the rupture the sections remain flat (Bernoulli hypothesis), (ii) The specific maximum shortening of the concrete is 0,0035, (iii) The specific maximum stretching for tensile reinforcement is 0,01, (iv) The specific maximum stretching reinforcement is 0,0148, (v) The steel and fiber stress-strain is linear until a value given by the ratio between yield stress and material linear elasticity modulus. Above that deformation, the stress is constant, (vi) the beam to be reinforced has no previous deformation, (vii) the beam did not suffer plastic deformation, or damage before submitted to the reinforcement.

The proposed methodology will evaluate the beams behavior in function of curvature (φ) according to equation 1, using the complete concrete stress-strain diagrams according to the

Figure 1 – Type of structure where was developed the numerical model

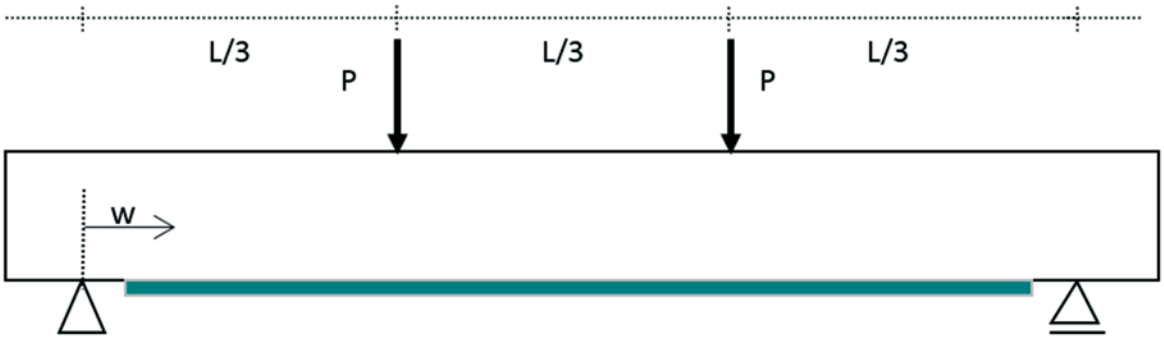

recommendations of NBR-6118 and fib and guidelines of (NBR-7480, [25]). This analysis was made by applying the reverse path in these project situations. It is considered as reverse path the external moment determination, arbitrating a specific deformation for the longest fiber of the concrete (ε_c). In this process, it is considered the compatibility of deformations (linear deformations), reinforcement deformations, steel and fiber are determined as a function of neutral line (x), variable presented on figure 2 and, consequently the tensile and compression strengths by the equation of balance forces.

$$\varphi = \frac{\varepsilon_c}{x} \quad (1)$$

The model that it is presented on results and discussions and primordially consists in determination of the neutral line position taking into consideration a specific concrete deformation (ε_c). That variable is necessary to evaluate the applied moment on the beam to determine the deformation. To the determination of the neutral line, was utilized the equation of balance forces of tensile and compression in the required section from the pure bending moment. The figure 1 presents type of reinforced beam whose numerical model was developed. The reinforcement is assessed on the section that it is more likely to bend (central section where the shear stress is null). The figure 2 presents a transversal section that it is characteristic of the beam reinforced to tensile strength (beam originally with lack of tensile reinforcement). C1 and C2 are compression's components from steel and compressed concrete, respectively. T1 and T2 are tensile components respectively from steel and the strengthening. On the same figure is presented the stress-strain diagram from NBR-6118 for the compressed concrete and from fib. Item 3 shows the detailed equations for both models and present stress-strain curves for few concrete types.

Figure 2 – Features of transversal rectangular cross section. Representation of the acting forces on a cross section with a differential thickness dz and the stress-deformation diagrams by NBR-6118 and *fib*

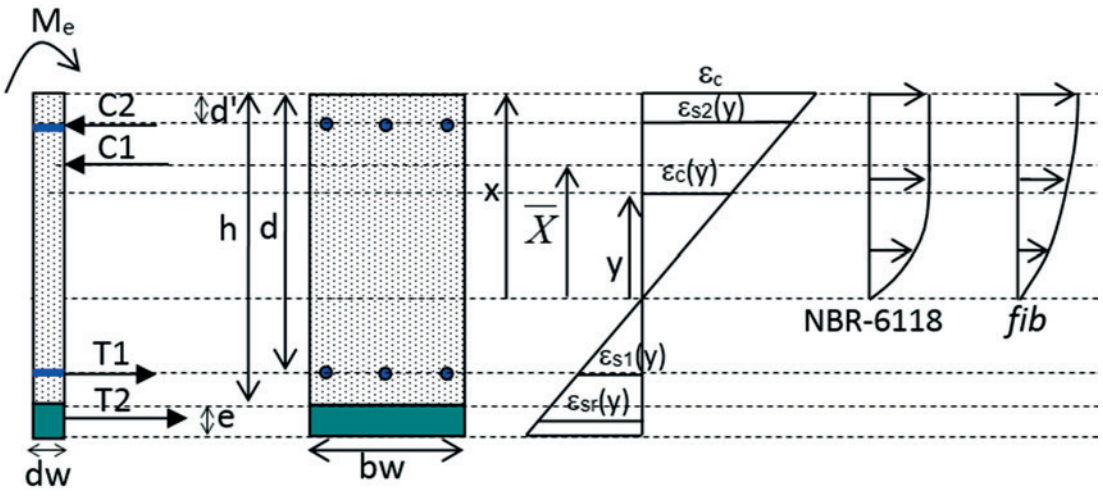

In Figure 2, ε_c represents a specific deformation from the most compressed concrete fiber, $\varepsilon(y)$ the specific deformation in function of the distance from the neutral line and x the neutral line height. The equation of balance forces (equation 2) can be utilized to determine the neutral line position. In this situation, the variable of interest remains implicit in the equation of single variable (the neutral line position). The equations solution is determined by numerical methods. To obtain other points to build the curve of moment-curvature, will be stipulated another specific deformations for the concrete, respecting the interval of [0; 0,0035]. In this process also must be respected the specific deformations limits for steel and structural reinforcement that was considered, respectively, 0,01 and 0,0148. Once the neutral line position is determined, it's also determined the stress and deformations of each material that composes the transversal section and it can be determined the applied moment to the structure that resulted on the specific deformation of the concrete ε_c adopted.

The equation to determination of the neutral line is generated from the solution of the equation 2 that it is written on general form where C1 is the concrete's compress force, C2 is the compress force of the compressed steel, T1 is the tensile force of the tensioned steel and T2 is the reinforcement's tensile force.

$$C1 + C2 - T1 - T2 = 0 \quad (2)$$

The equation 2 also can be written on stress and area forms resulting on equation 3. The solution of the equation 3, according to what was studied in the development, is an iterative form in function of specific deformation of arbitrated concrete. On equation 3, (σ_c and A_c), respectively, is the stress and the area of compressed concrete; (σ_{S2} and A_{S2}), respectively, is the stress and the superior reinforcement area; (σ_{S1} and A_{S1}), respectively, is the stress and the area of the inferior reinforcement; (σ_{sr} and A_{Sr}), respectively, is the stress and strengthening area.

$$\sigma_c A_c + \sigma_{s2} A_{s2} = \sigma_{s1} A_{s1} + \sigma_{sr} A_{sr} \quad (3)$$

Once the neutral line position (x) is estimated, and as ε_c (adopted value) is known, all the other deformations are determined and, consequently the forces C1, C2, T1 and T2. Based on this forces it can be calculated the external moment that occasioned the deformation ε_c through equation 4, where the moment is calculated based on the section's base. In equation 4, $\overline{X}$ is the centroid of the concrete compressed area.

$$M_e = C1 \cdot \left(\overline{X} + h - x + e\right) + C2 \cdot \left(h - d' + e\right) - T1 \cdot (h - d + e) - T2 \cdot \left(\frac{e}{2}\right) \quad (4)$$

In the "T" cross section beam scenario the process is analogue to beams with rectangular cross section. The figure 3 that have presented a "T" cross section with a determined characteristic load and the principal variables utilized on the model. The equation for

Figure 3 – Features of transversal "T" type cross section. Representation of the acting forces in a cross section with differential thickness dz and the stress-deformation diagrams by NBR-6118 and *fib*

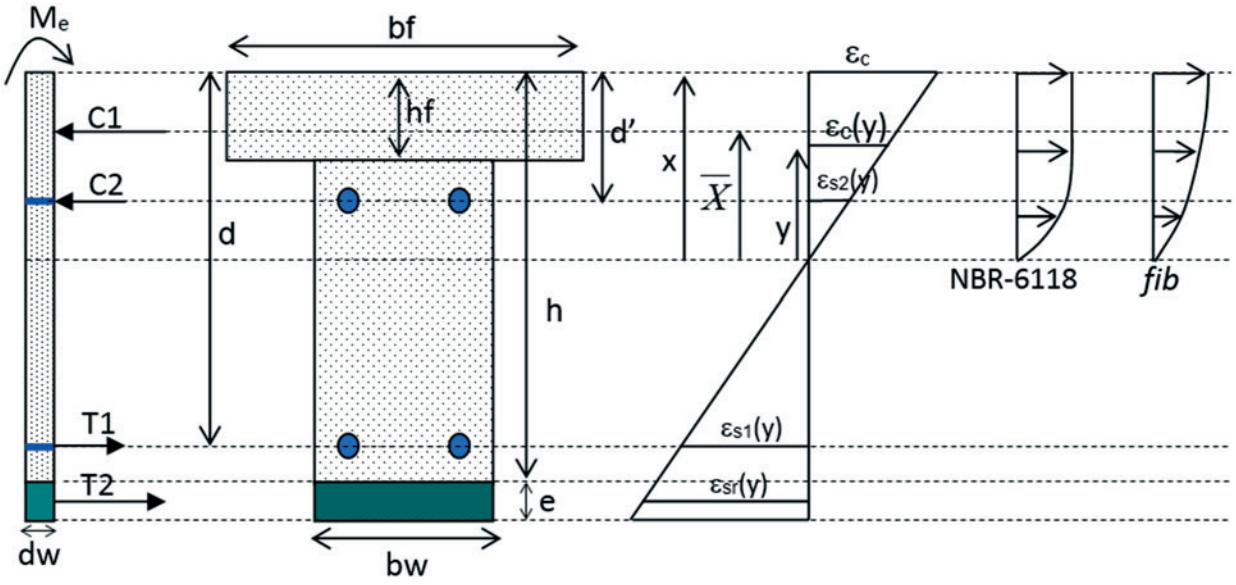

the determination of a neutral line and, after that an equation to determine the applied external moment it is given by the same equations 2 and 4 of a rectangular cross section, but here it can be adopted the nomenclature of figure 3, in the words:

3. Results and discussions

In this section of the paper will be presented the equations that compose models to determination of a function moment-curvature considering rectangular and "T" cross section beams as well as the NBR-6118 and fib codes.

On the equation of balance forces (equation 3), it is known that the stress on steel (compression and tensile) and the stress on strengthening are linear functions of deformation and depends only from the specific deformation of concrete, which is arbitrated on each step (or on each specific deformation of the fiber's concrete that it is most compressed, ε_c). It was considered that the steel and the strengthening have linear deformation behavior until reaches ε_k given by equation 5, where f_k is the stress and E_k the elasticity modulus. The variables (ε_k, f_k, and E_k) take place, respectively, (ε_{s1}, f_{s1} and E_s), for the tensioned steel, (ε_{s2}, f_{s2} and E_s), for the compressed steel and (ε_{cr}, f_{cr} and E_r), for the strengthening. Figure 8 presents the stress and elasticity modulus values applied in this study. The maximum specific deformation for these materials (steel and strengthening) were, respectively, 0,01 and 0,0148 according to technical recommendations. Moreover, for steel (ε_k<ε<0,01) and for strengthening (ε_k<ε<0,0148), the stress f_k was considered.

$$\varepsilon_k = \frac{f_k}{E_k} \tag{5}$$

Equation 6 shows the specific deformation of the superior reinforcement, inferior reinforcement and strengthening, being all function of neutral line distance, as represented in figure 2 and 3. These equations show the case of compression on the superior reinforcement and tensile stress in the inferior reinforcement.

Figure 4 – Diagram (σ - ε) concrete (NBR-6118)

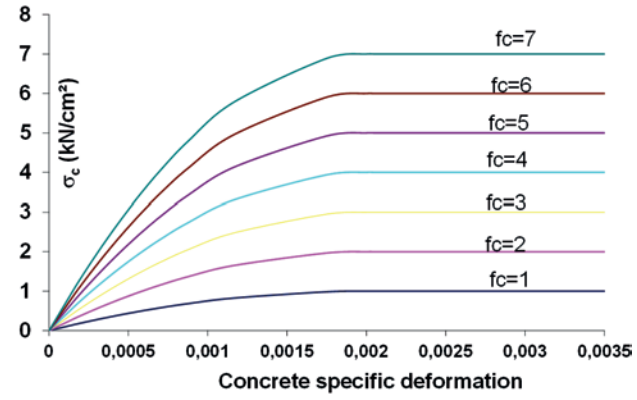

There are cases (function of neutral line position) that both are reinforcement of tensile stress or reinforcement of compression stress, the only difference is that the respective equation must me multiplied by (-1).

$$\begin{cases} \varepsilon_{s2}(x) = \dfrac{\varepsilon_c (x - d')}{x} \text{ compression} \\ \varepsilon_{s1}(x) = \dfrac{\varepsilon_c (d - x)}{x} \text{ tensile} \\ \varepsilon_{sr}(x) = \dfrac{\varepsilon_c \left(h - x + \dfrac{e}{2} \right)}{x} \text{ tensile} \end{cases} \tag{6}$$

From the specific material deformation, stresses are obtained by equation 7 and the components of each force are obtained respectively by the multiplication of its transversal section.

$$\sigma_k(x) = E_k \varepsilon_k(x) \tag{7}$$

The stress in the concrete depends of a nonlinear function of deformation as recommended by NBR-6118 and *fib*. The stress deformation diagram proposed by NBR-6118 is presented in equation 8 that considers two sections according to specific deformation of the concrete's most compressed fiber (ε_c), being one curve section given by equation 8 and one section with constant stress for the specific deformation interval of 0,002<ε_c ≤0,0035 and exactly the same as f_c stress (simple concrete compression stress). Figure 4 presents stress-strain curves obtained from equation 8 for concrete.

$$\sigma_c = f_c \left[1 - \left(1 - \frac{\varepsilon_c}{0{,}002} \right)^2 \right] \tag{8}$$

Considering the modelling through fib recommendation, it generates the equations 9, 10, 11 and 12, which compounds fib recommendation of the stress-strain diagram.

$$\sigma_c = \frac{\dfrac{E_{ci}\varepsilon_c}{E_{c,\sec}\varepsilon_{co}} - \left(\dfrac{\varepsilon_c}{\varepsilon_{co}} \right)^2}{1 + \left(\dfrac{E_{ci}}{Ec,\sec} - 2 \right) \dfrac{\varepsilon_c}{\varepsilon_{co}}} f_{cm} \tag{9}$$

$$\varepsilon_{co} = 0{,}0017 + 0{,}0010 \left(\frac{f_{cm}}{f_{cmo}} \right) \tag{10}$$

$$E_{ci} = \alpha_E E_{co} \left(\frac{f_{cm}}{f_{cmo}} \right)^{\frac{1}{3}} \quad (11)$$

$$E_{c,\sec} = \frac{f_{cm}}{\varepsilon_{co}} \quad (12)$$

Equations 9, 10, 11 and 12 provide: $E_{ci,}$ which is the elasticity modulus tangent when σ_c=0 [MPa] for concrete age of 28 days; E_{co}=2,15. 10^4 Mpa, $f_{cm,}$ which is the average compression stress; f_{cmo} = 10 MPa; α_E is the coefficient that depends on material found in the concrete, in this case, basalt, α_E=1,2.

Figure 5 presents stress-strain diagram for fib recommendation for values of concrete resistance features. It is observed that the diagram is built on a continuous curve for the concrete specific deformation interval $0 \leq \varepsilon_c \leq 0{,}0035$.

The proposed analytical model for concrete compression determination is done considering the stress-strain diagram on NBR-6118 and *fib* without simplifications, which implies on the necessity of usage of convergence numerical method of equations 2 or 3 on each step (each ε_c adopted). After determined the neutral line position, it is necessary to determine the area of compressed concrete centroid to calculate the resistant moment, which, analytically, resulted in the deformation initially arbitrated. The difficulties to formulate the algorithm are strongly influenced by the nonlinear concrete's behavior. For a generic beam of a transversal section with width b_w, the equations 13 and 14 show respectively and from a generalized perspective, how concrete compression component (term from equation 2) and centroid of the compressed concrete region (equation's 4 variable) are obtained, being F_{cc} the component of concrete compression and dy the integration element. The equation 15 shows the concrete's deformation of a random fiber in function of this fiber positioning according to the nomenclature adopted on figures 2 and 3.

Figure 5 – Diagram (σ - ε) concrete (*fib*)

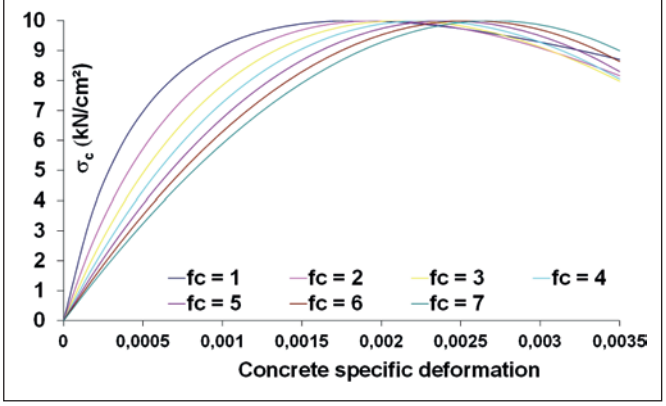

$$C1 = F_{cc} = \left[\int_0^x (\sigma_c b_w) dy \right] \quad (13)$$

$$\overline{X} = \frac{\int_0^x (\sigma_c b_w y) dy}{\int_0^x (\sigma_c b_w) dy} \quad (14)$$

$$\varepsilon_c(y) = \frac{\varepsilon_c \, y}{x} \quad (15)$$

The considered model to predict limit stress in terms of concrete strengthening adherence was based on model proposed by (Chen and Teng [26]) and modified by (Beber [6]). Equation 16 presents the model applied, where "e" is the strengthening thickness and $\sigma_{r,\max}$ the stress limit to adherence of concrete reinforcement.

$$\sigma_{r,\max} = 0{,}1956 \sqrt{\frac{E_r \sqrt{f_c}}{e}} \quad [\text{kN/cm}^2] \quad (16)$$

3.1 Model for rectangular cross section beams - NBR- 6118

For the generation of the resultant equation of compression force and centroid of the compressed region, was utilized equation 17, which is originated from equation 8 but modified to consider the integration variable y, as shown in equation 15.

$$\sigma_c = f_c \left[1 - \left(1 - \frac{\varepsilon_c \cdot y}{0{,}002x} \right)^2 \right] \quad (17)$$

Due to these the two diagram sections, 2 different cases are possible:

Case 1: for $\varepsilon_c \leq 0{,}002$

In this case the maximum specific deformation of the most compressed concrete fiber is limited in 0,002, in other words, the concrete deformation in the entire compressed area is placed at the curve section. Equations 18 and 19 show, respectively, compression resultant force and concrete centroid obtained from equations 13 and 14.

$$F_{cc} = b_w f_c x \left[500\varepsilon_c - \frac{250000}{3} \varepsilon_c^{\,2} \right] \quad (18)$$

Figure 6 – Flowchart of the possible group of equations to determine the pair moment - curvature, according to the specific deformation of the concrete in the most compressed fiber and the neutral line position

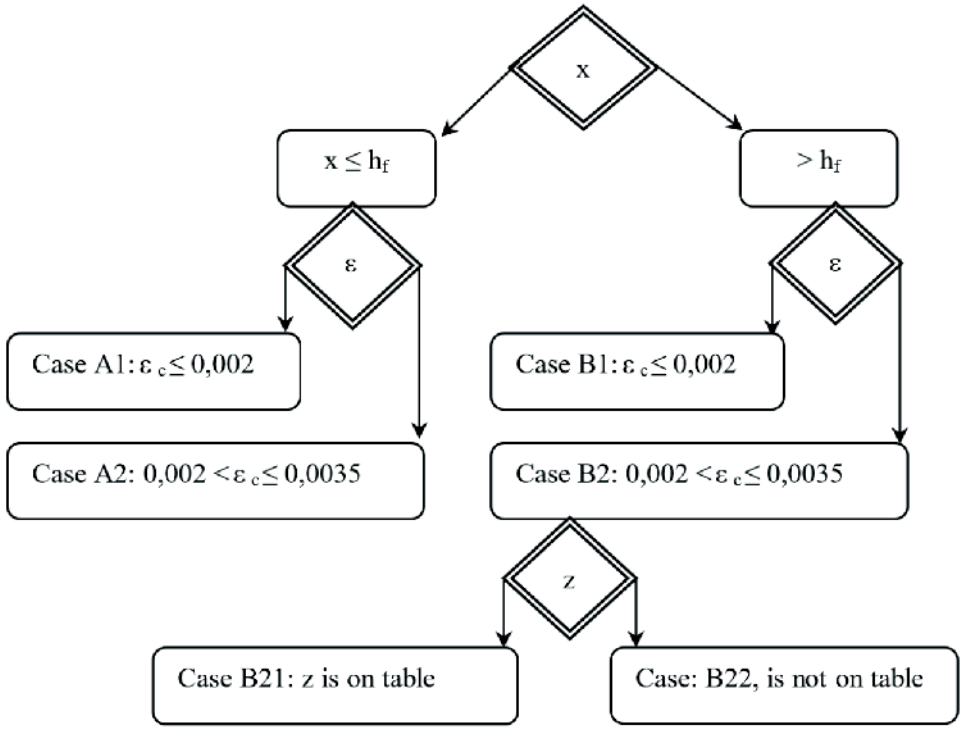

$$\overline{X} = \frac{x(10 - 1875\varepsilon_c)}{15 - 2500\varepsilon_c} \quad (19)$$

Case 2: for ε_c > 0,002

In this case the maximum specific deformation of the most compressed concrete fiber has a superior value of 0,002, in other words, concrete deformation might be placed at the curve section as wells as the constant section. Equation 20 and 21 show, respectively, compression resultant force and concrete centroid.

$$F_{cc} = \left[\int_0^{\frac{0,002}{\varepsilon_c}x} (\sigma_c b_w)dy\right] + xb_w f_c\left(1 - \frac{0,002}{\varepsilon_c}\right) = b_w f_c x\left[1 - \frac{1}{1500\varepsilon_c}\right] \quad (20)$$

$$\overline{X} = \frac{x\left[\frac{1}{2} - \frac{1}{3000000\varepsilon_c^{\,2}}\right]}{\left[1 - \frac{2}{3000\varepsilon_c}\right]} \quad (21)$$

3.2 Model for "T" cross section beams - NBR-6118

In the "T" cross section scenario, as a composed section, several cases are possible by matching with deformations ε_c greater and lower than 0,002. Many possible cases are presented in the flowchart of figure 6. Next, will be described equations for the compressive area of the concrete and for the matching centroid on each case. The distance from neutral line to the concrete specific deformation is designated as z, whose value is 0,002.

Case A1: for $x \leq h_f$ and $\varepsilon_c \leq 0,002$

This scenario is where the neutral line position is on table and the deformation of the concrete in the most compressed fiber is lower than 0,002. The equations that have compression components for concrete and centroid either, are represented in equations

22 and 23, respectively, and were obtained by equations 13 and 14.

$$F_{cc} = b_f f_c x\left[500\varepsilon_c - \frac{250000}{3}\varepsilon_c^{\,2}\right] \quad (22)$$

$$\overline{X} = \frac{x\left(10 - 1875\,\varepsilon_c\right)}{15 - 2500\,\varepsilon_c} \quad (23)$$

Case A2: for $x \le h_f$ and $0{,}002 < \varepsilon_c \le 0{,}0035$

This scenario is where the neutral line position is on table and the concrete specific deformation in the most compressed fiber is in the range of 0,002 to 0,0035. The equations that have components of compression for concrete and centroid either, in this scenario, are represented in equations 24 and 25, respectively.

$$F_{cc} = \left[\int_0^{\frac{0{,}002}{\varepsilon_c}x} \left(\sigma_c b_f\right)dy\right] + b_f f_c\left(\frac{0{,}002}{\varepsilon_c}x\right) \rightarrow F_{cc} = b_f f_c x\left[1 - \frac{1}{1500\varepsilon_c}\right] \quad (24)$$

$$\overline{X} = \frac{x\left[\frac{1}{2} - \frac{1}{3000000\varepsilon_c^{\,2}}\right]}{\left[1 - \frac{2}{3000\varepsilon_c}\right]} \quad (25)$$

Case B1: for $x > h_f$ and $\varepsilon_c \le 0{,}002$

This scenario is where the neutral line position is under table and the concrete specific deformation in the most compressed fiber is lower or equal to 0,002. The equations that have components of compression for concrete and centroid either, for this scenario, are represented in equations 26 and 27, respectively.

$$F_{cc} = b_w\int_0^x \sigma_c dy + \left(b_f - b_w\right)\int_{x-h_f}^x \sigma_c dy$$

$$F_{cc} = b_w f_c x\left[500\varepsilon_c - \frac{250000}{3}\varepsilon_c\right] + \left(b_f - b_w\right)f_c\alpha$$

$$\alpha = \left[500\varepsilon_c x - \frac{250000}{3}\varepsilon_c^{\,2}x - \frac{500\varepsilon_c\left(x-h_f\right)^2}{x} + \frac{250000}{3x^2}\varepsilon_c^{\,2}\left(x-h_f\right)^3\right] \quad (26)$$

$$\overline{X} = \frac{x(10 - 1875\varepsilon_c)}{15 - 2500\varepsilon_c} \quad (27)$$

Case B21: for $x > h_f$ and $0{,}002 < \varepsilon_c < 0{,}0035$ and z is on table

There are 3 (three) required conditions for this scenario, the neutral line position under table, the specific deformation of the concrete on the most compressed fiber that will be in the range of 0,002 to 0,0035. Furthermore, the distance from the neutral line position to the deformation has to be 0,002, designated as z and situated on table. The equations that have compression components for concrete and centroid either, for this scenario, are represented in equations 28 and 29, respectively.

$$F_{cc} = b_w\int_0^z \sigma_c d_y + b_w f_c\left(x-z\right) + \left(b_f - b_w\right)\int_{x-h_f}^z \sigma_c dy + \left(b_f - b_w\right)f_c\left(x-z\right)$$

$$F_{cc} = b_w f_c\beta + \left(b_f - b_w\right)f_c\delta$$

$$\beta = \left[500\varepsilon_c\frac{z^2}{x} - \frac{250000\varepsilon_c^{\,2}z^3}{3x^2} + x - z\right]$$

$$\delta = \left[\frac{500\varepsilon_c z^2}{x} - \frac{250000\varepsilon_c^{\,2}z^3}{3x^2} - \frac{500\varepsilon_c\left(x-h_f\right)^2}{x} + \frac{250000\varepsilon_c^{\,2}\left(x-h_f\right)^3}{3x^2} + x - z\right] \quad (28)$$

$$\overline{X} = \frac{x\left[\frac{1}{2} - \frac{1}{3000000\varepsilon_c^{\,2}}\right]}{\left[1 - \frac{2}{3000\varepsilon_c}\right]} \quad (29)$$

Case B22: for $x > h_f$ and $0{,}002 < \varepsilon_c \le 0{,}0035$ and z is not on table

There are 3 (three) required conditions for this scenario, the neutral line position under table, the specific deformation of the concrete in the most compressed fiber that will be in the range of 0,002 to 0,0035. Furthermore, the distance from the neutral line position to the deformation has to be 0,002, designated as z and situated under table. The equations that have compression components for concrete and centroid either, for this scenario, are represented in equations 30 and 31, respectively.

$$F_{cc} = b_w\int_0^z \sigma_c dy + b_w f_c\left(x-z\right) + \left(b_f - b_w\right)f_c h_f$$

$$F_{cc} = b_w f_c\left[500\varepsilon_c\frac{z^2}{x} - \frac{250000\cdot\varepsilon_c^{\,2}z^3}{3x^2} + x - z\right] + \left(b_f - b_w\right)f_c h_f \quad (30)$$

$$\overline{X} = \frac{x\left[\frac{1}{2} - \frac{1}{3000000\varepsilon_c{}^2}\right]}{\left[1 - \frac{2}{3000\varepsilon_c}\right]} \quad (31)$$

3.3 Model for rectangular cross section beams - fib

The equations 32 and 33 were obtained through the generic equations 13 and 14, and the model proposed by *fib* (equations 9, 10, 11 and 12), in which equation 32 is for compressive strength and equation 33 is for the centroid of the concrete compressed area.

$$F_{cc} = b_w f_{cm}\left[c\left(\frac{x}{d} - \frac{\ln(x.d+1)}{d^2}\right) - e\left(\frac{(x.d+1)^2}{2d^3} - \frac{2(x.d+1)}{d^3} + \frac{\ln(x.d+1)}{d^3} + \frac{3}{2d^3}\right)\right] \quad (32)$$

$$\overline{X} = \frac{\frac{c}{d^3}[\varphi] - \frac{e}{d^4}[\gamma]}{c\left(\frac{x}{d} - \frac{\ln(x.d+1)}{d^2}\right) - e\left(\frac{(x.d+1)^2}{2d^3} - \frac{2(x.d+1)}{d^3} + \frac{\ln(x.d+1)}{d^3} + \frac{3}{2d^3}\right)}$$

$$\varphi = \left[\frac{(x.d+1)^2}{2} - 2(x.d+1) + \ln(x.d+1) + \frac{3}{2}\right]$$

$$\gamma = \left[\frac{(x.d+1)^3}{3} - 3\frac{(x.d+1)^2}{2} + 3(x.d+1) - \ln(x.d+1) - \frac{11}{6}\right] \quad (33)$$

The parameters a, c, d, e are described below, in equations 32 and 33.

$$a = \frac{E_{ci}}{f_{cm}} \qquad c = \frac{a\varepsilon_c}{x} \qquad d = \frac{1}{x}\left(a\varepsilon_c - \frac{2\varepsilon_c}{\varepsilon_{co}}\right) \qquad e = \frac{\varepsilon_c{}^2}{x^2\varepsilon_{c0}{}^2}$$

3.4 Model for "T" cross section beams - fib

For this "T" cross section and considering *fib* guidelines there are 2 (two) cases which depend on the neutral line position (below or above the table).

Case 1: for x ≤ h_f, in other words, neutral line on table

In this case, the neutral line position (x) is considered as placed on table (h_f). The components for compressive strength of the concrete and compressive centroid area are represented in equations 34 and 35, respectively. The coefficients (a, c, d, e) are the same in case 3.3.

$$F_{cc} = b_f f_{cm}\left[c\left(\frac{x}{d} - \frac{\ln(x.d+1)}{d^2}\right) - e\left(\frac{(x.d+1)^2}{2d^3} - \frac{2(x.d+1)}{d^3} + \frac{\ln(x.d+1)}{d^3} + \frac{3}{2d^3}\right)\right] \quad (34)$$

$$\overline{X} = \frac{\frac{c}{d^3}[\eta] - \frac{e}{d^4}[\lambda]}{c\left(\frac{x}{d} - \frac{\ln(x.d+1)}{d^2}\right) - e\left(\frac{(x.d+1)^2}{2d^3} - \frac{2(x.d+1)}{d^3} + \frac{\ln(x.d+1)}{d^3} + \frac{3}{2d^3}\right)}$$

$$\eta = \left[\frac{(x.d+1)^2}{2} - 2(x.d+1) + \ln(x.d+1) + \frac{3}{2}\right]$$

$$\lambda = \left[\frac{(x.d+1)^3}{3} - 3\frac{(x.d+1)^2}{2} + 3(x.d+1) - \ln(x.d+1) - \frac{11}{6}\right] \quad (35)$$

Case 2: for x > h_f, in other words, neutral line under table

In this case, the neutral line position (x) is considered as placed below the table (h_f). The components for compressive strength of the concrete are represented in equation 36, and the parameters a, c, d, e are the same coefficients presented in case 3.3.

$$F_{cc} = (A - B)b_w f_{cm} + P(b_f - b_w)f_{cm} - Q(b_f - b_w)f_{cm} \quad (36)$$

Where:

$$A = c\left(\frac{x}{d} - \frac{\ln(x.d+1)}{d^2}\right)$$

$$B = e\left(\left(\frac{(x.d+1)^2}{2d^3}\right) - \frac{2(x.d+1)}{d^3} + \frac{\ln(x.d+1)}{d^3} + \frac{3}{2d^3}\right)$$

$$P = \left[-\frac{(x-h_f)}{d} + \frac{\ln((x-h_f)d+1)}{d^2}\right]c + A$$

$$Q = \left[\frac{-3}{2d^3} - \frac{((x-h_f)+1)^2}{2d^3} + \frac{2((x-h_f)d+1)}{d^3} - \frac{\ln((x-h_f)d+1)}{d^3}\right]e + B$$

The equation for centroid in the concrete compressed area is given by equation 37, and parameters (a, c, d, e) are the same presented on item 3.3.

$$\overline{X} = \frac{\frac{c}{d^3}[\zeta] - \frac{e}{d^4}[\psi]}{c\left(\frac{x}{d} - \frac{\ln(x.d+1)}{d^2}\right) - e\left(\left(\frac{(x.d+1)^2}{2d^3}\right) - \frac{2(x.d+1)}{d^3} + \frac{\ln(x.d+1)}{d^3} + \frac{3}{2d^3}\right)}$$

$$\zeta = \left[\frac{(x.d+1)^2}{2} - 2(x.d+1) + \ln(x.d+1) + \frac{3}{2}\right]$$

$$\psi = \left[\frac{(x.d+1)^3}{3} - 3\frac{(x.d+1)^2}{2d^4} + 3(x.d+1) - \ln(x.d+1) - \frac{11}{6}\right] \quad (37)$$

3.5 Model consistence

In order to evaluate the model consistency, some experimental results were compared to others obtained through the model. These results were published in (Beber et al., [5]) and in (Andreolli, et al., [18]). Is not part of this work to perform these tests, as it were obtained through these publications. The experimental program that acquired these experimental data was performed by Tests and Structural Models Laboratory (*Laboratório de Ensaios e Modelos Estruturais*-LEME) from the Graduate Program in Civil Engineering at Federal University of Rio Grande do Sul, and consisted in performing ten prototypes of reinforced concrete beams according to figure 7 and 8 (Beber et al. [5]).

The concrete specific deformation, reinforcement and strengthening strips, in the central cross section of each prototype were measured through strain gages. The applied load determination was performed through a load cell with a capacity of 200kN. The vertical displacements were determined through vertical registers, with a precision of 0,01 mm, in the load application point and the central section. The horizontal displacements were measured in the roller support. The flowchart, presented on figure 8, has an input data in the numerical model according to the nomenclature used in the present study.

The results acquired in rupture tests and theoretical data obtained through the proposed model are presented in table 1, showing great similarity.

To obtain the theoretical rupture load in table 1 was used equation 38 that is originated from diagram of bending moment between the 2 (two) sections of load application, as M_e the resulting external moment in the cross section, according to equation 4. The types of rupture are classified as type 1, 2 and 3. Type 1, rupture through excessive tensile strength on steel; Type 2, rupture through excessive tensile strength on the strengthening; and type 3, rupture through adherence failure between concrete and strengthening.

$$\text{carga} = \frac{6M_e}{L} \qquad (38)$$

A parametric study was performed to evaluate the behavior on the function moment - curvature changing the amount of strengthening, codes, types of section and the material features that composes the beams (concrete and steel). An embracing parametric study was based on (Andreolli et al., [18]). The results for a rectangular cross section are presented on figure 9, while figure 10 present the results for a "T" cross section. Both codes considered have shown great match between them and the curves are practi-

Figure 7 – Test scheme and prototype detailing (Beber, et al. (5))

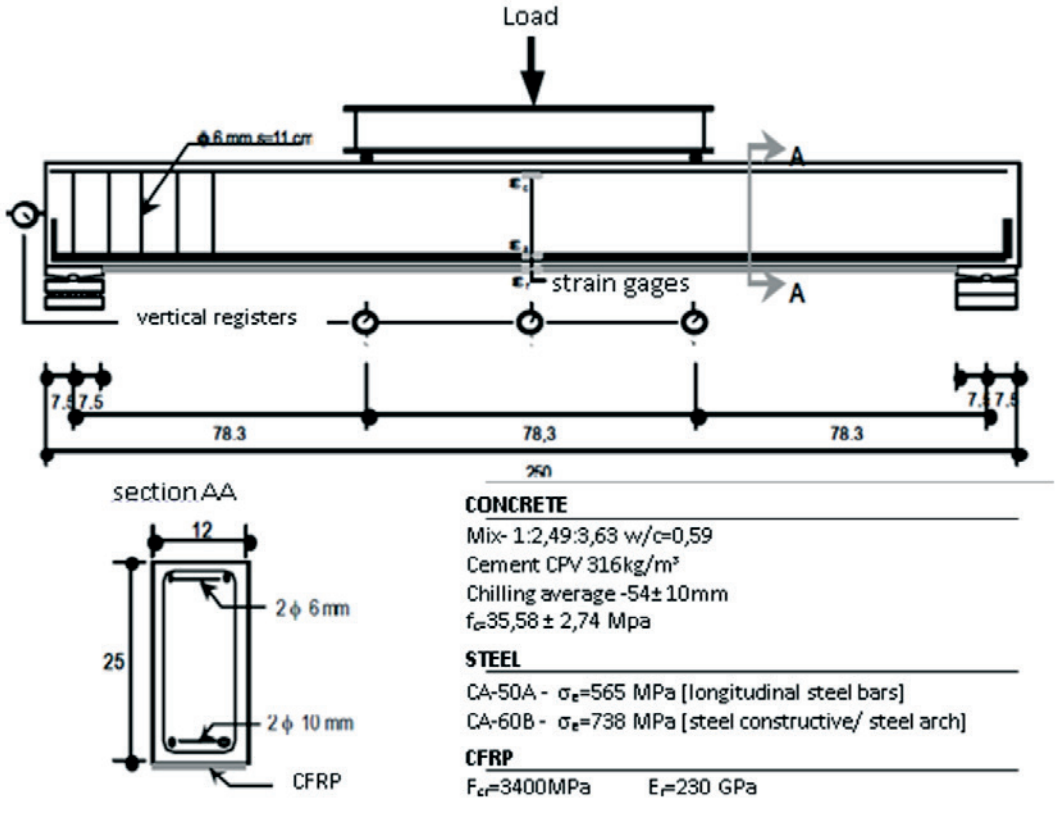

Figure 8 – Data from tested beams in lab

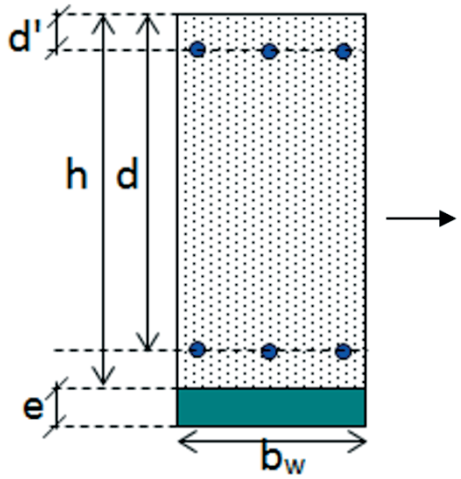

Tested beams data	
Variable	Value
b_w [cm]	12
d [cm]	22,4
d' [cm]	2
f_{cr}[kN/cm²]	340 (fiber)
f_{s2} [kN/cm²]	73,8(steel compression)
f_{s1} [kN/cm²]	56,5 (steel tensile)
f_c [kN/cm²]	3,36 (concrete)
A_{s2} [cm²]	0,52 (compression)
A_{s1}[cm²]	1,57 (tensile)
e[cm]	0,011 by layer
E_r [kN/cm²]	23000 (fiber)
E_s [kN/cm²]	21000 (steel)
L [cm]	235

cally overlapped. For the case of beams with T cross section was considered the parameters on figure 8 including a table with height h_f=5cm and width b_f=20cm.

4. Conclusion

The strengthening of reinforced concrete beams with carbon fiber composites is an interesting alternative in several situations, due to, mainly, its practicality to perform and quickness. However, to achieve strengthening efficiency, it is necessary to exist sufficient adherence area, and does not occur rupture on the compressed concrete. If compared to the experimental results, the theoretical model have presented very effective results, which corroborate to evaluate the reinforced concrete beams strengthened with carbon fiber composites or steel plates. The curvature in the structural beam can be evaluated through the proposed model in function of the acting moment and may evaluate the efficiency to add more strengthening layers. The numerical model proposed shown that NBR-6118 and *fib* guidelines presented accurate results to the moment - curvature and to the load rupture. The proposed methodology appears to be an interesting tool in order to evaluate the strengthening performance, as well as to evaluate the structure load capacity. It is recommended

Table 1 – Theoretical and experimental results in comparison. (Adapted from Beber, et al. (5) and Andreolli, et al. (18))

Beam	Strengthening	Experimental results		Theoretical results			
		Failure mode	Load of rupture (kN)	Load of rupture NBR (kN)	Difference (%)	Load of rupture fib (kN)	Difference (%)
1	–	type 1	47,0	49.18 (type 1)	4,19	49,03 (tipo 1)	3,88
2	–	type 1	47,4				
3	1 layer	type 1	65,2	67,31 (type 1)	5,83	67,47 (type 1)	6,08
4	1 layer	type 2	62,0				
5	4 layers	type 3	102,2	116,18 (type 3)	14,58	116,67 (type 3)	15,06
6	4 layers	type 3	100,6				
7	7 layers	type 3	124,2	130,76 (type 3)	5,37	123.65 (type 3)	0,36
8	7 layers	type 3	124,0				
9	10 layers	type 3	129,6	128,94 (type 3)	3,38	124,72 (type 3)	6,88
10	10 layers	type 3	137,0				

Figure 9 – Function moment - curvature for beams with rectangular cross section taking in comparison NBR-6118 and *fib* codes. About nomenclature, 2 C NBR Ret means that has 2 strengthening layers, NBR code and rectangular cross section

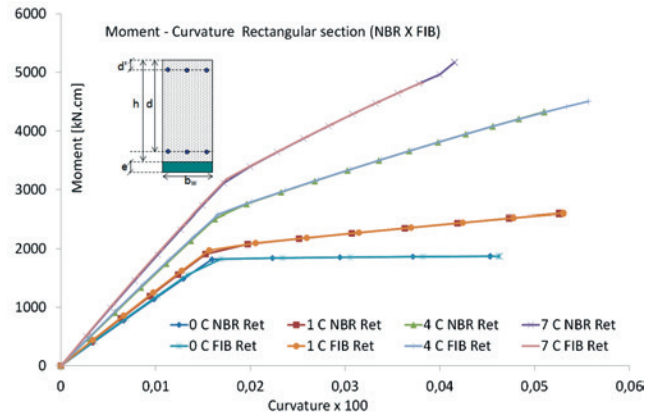

Figure 10 – Function moment - curvature for beams with "T" cross section taking in comparison NBR-6118 and *fib* codes. About nomenclature, 7 C FIB T means that has 7 strengthening layers, *fib* code and "T" cross section

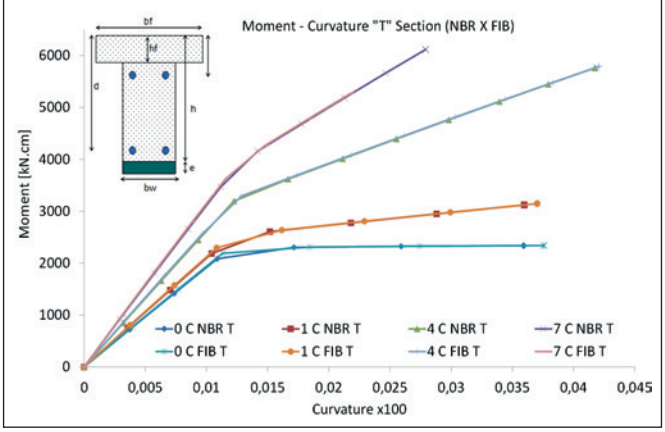

to develop models and experiments that incorporate data from the loading start until the beam breaks, in order to evaluate the model performance at any deformation domain.

5. Bibliographic references

[1] SPAGNOLO JR, L. A., SÁNCHEZ FILHO, E. S., VELASCO, M. S. L. RC T beams strengthened to shear with carbon fiber composites, 2013. IBRACON Structural Journal, SP, v. 6, n. 1, p. 1-12, 2013.

[2] SAADATMANESH, H., EHSANI, M. R. RC beams strengthened with GRFP plates. I: experimental study. Journal of Structural Engineering, New York, ASCE, v.117, n.11, p.3417-3433, 1991.

[3] AN, W., SAADATMANESH, H., EHSANI, M. R. RC beams strengthened with GRFP plates. II: analysis and parametric study. Journal of Structural Engineering, New York, ASCE, v.117, n.11, p.3435-3455, 1991.

[4] GARCÉS, P., ZORNOZA, E., E. ALCOCEL, G., GALAO, Ó. ANDIÓN, L.G. Mechanical properties and corrosion of CAC mortars with carbon fibers. Construction and Building Materials v. 34, p. 91–96, 2012.

[5] BEBER, A. J., CAMPOS F. A., CAMPAGNOLO, J. L. Reinforced concrete beam structures with carbon fiber post-impregnated material . Téchne. Revista de Tecnologia da Construção, SP, n. 45, p. 52-55, 2000.

[6] BEBER, A. J. Structural behavior of reinforced concrete beams with carbon fiber composites. 2003. 317 p. Thesis (Doctorate in Civil Engineering) - UFRGS.

[7] GARCEZ, M. R., QUININO, U. C. M.., SILVA FILHO, L. C. P., MEIER, U. Application of Heat-Activated Films as a new generation of adhesives used for bonding Fiber Reinforced Polymers to concrete., IBRACON Structural Journal, SP, v. 1, n. 4, p. 393-420, 2008.

[8] FERRARI, V. J., HANAI, J. B. Flexural strengthening of reinforced concrete beams with carbon fibers reinforced polymer (CFRP) sheet bonded to a transition layer of high performance cement-based composite, 2012. IBRACON Structural Journal, SP, v. 5, n. 5, p. 596-626, 2012.

[9] TIAN, H., ZHANG, Y.X., YE, L., YANG, C. Mechanical behaviours of green hybrid fibre-reinforced cementitious composites. Construction and Building Materials, v. 95 p. 152–163, 2015.

[10] SANTOS, G. S., NICÁCIO, W. G., LIMA, A. W., MELO, G. S. S. A. Punching strengthening in flat plates of reinforced concrete with carbon fiber reinforced polymer (CFRP). IBRACON Structural Journal, SP, v. 7, n. 4, p.592-695, 2014.

[11] GAMINO, A. L., SOUSA, J. L. A. O., MANZOLI O. L., BITTENCOURT, T. N. R/C structures strengthened with CFRP part II: analysis of shear models. IBRACON Structural Journal, SP, v. 3, n. 1, p. 24-49, 2010.

[12] GARCEZ, M. R., SILVA FILHO, L. C. P., MEIER, U.R.S. Post-strengthening of reinforced concrete beams with prestressed CFRP strips. Part 1: Analysis under static loading. IBRACON Structural Journal, SP, v. 5, n. 3, p. 343-361, 2012.

[13] BEBER, A. J., CAMPOS F. A. CFRP Composites on the shear strengthening of reinforced concrete beams. IBRACON Structural Journal, SP, v. 1, n. 2, p. 127-143, 2005.

[14] YAQUB, M., BAILEY, C.G. Repair of fire damaged circular reinforced concrete columns with FRP composites, Construction and Building Materials v. 25, p. 359–370, 2011.

[15] SWAMY, R. M., JONES, R., BLOXHAM, J.W. Structural behavior of reinforced concrete beams strengthened by epoxy-bonded steel plates. Journal of Structural Engineering. v. 2, n. 65A , p.59-68, 1987.

[16] BONO, G. F. F., CAMPOS F. A., PACHECO, A. R. A 3D finite element model for reinforced concrete structures analysis. IBRACON Structural Journal, SP, v. 4, p. 548-560, 2011.

[17] GAMINO, A. L., BITTENCOURT, T. N., SOUSA, J. L. A. O.

R/C structures strengthened with CFRP Part I: analysis of flexural models. IBRACON Structural Journal, SP, v. 2, n. 4, p. 326-355, 2009.

[18] ANDREOLLI, I., BEBER, A. J., CAMPAGNOLO, J. L. Parametric study of structural strengthening of reinforced concrete beam with carbon fiber composites. DAMSTRUCT, 2000. Third international conference on the behavior of damaged structures. UFF-RJ, 2000.

[19] EL-REFAIE, S. A., ASHOUR, A. F., GARRITY, S. W. Flexural capacity of reinforced concrete beams strengthened with external plates. In: INTERNATIONAL CONFERENCE ON STRUCTURAL FAULTS AND REPAIR, 8. London. Proceedings. Edinburgh: Engineering Technics Press, CD-ROM, 1999.

[20] AL-SAIDY, A.H., KLAIBER, F.W., WIPF, T.J., AL-JABRI, K.S. AL-NUAIMI, A.S. Parametric study on the behavior of short span composite bridge girders strengthened with carbon fiber reinforced polymer plates, Construction and Building Materials v. 22 p. 729–737, 2008.

[21] HOLLAWAY, L.C., LEEMING, M.B. Strengthening of reinforced concrete structures using externally bonded FRP composites in structural and civil engineering. 1ed. Cambrifge: Woodhead Publishing Limited, 327p, 1999.

[22] AGBOSSOU, A., LAURENT M., LAGACHE, M., HAMELIN, P. Strengthening slabs using externally-bonded strip composites: Analysis of concrete covers on the strengthening, Composites: Part B 39, p. 1125–1135, 2008.

[23] NBR-6118. Design of concrete structures – procedure. ABNT-Code, Rio de Janeiro, 231 p, 2007.

[24] FÉDÉRATION INTERNATIONALE DU BÉTON. Structural concrete: textbook on behaviour, design, and perfomance. Lausanne, 1999, v.1 (Model Code 1990).

[25] NBR-7480. Bar and steel wires for reinforced concrete. ABNT-Code, Rio de Janeiro, 1996.

[26] CHEN, J. F., TENG, J. G. Anchorage strength models for FRP and steel plates bonded to concrete. Journal of Structural Engineering. N.Y, ASCE, v. 127, n. 7, p. 784-791, 2001.